Strut Analysis Applied to Stiffened Compression Panels

BY D. G. WILLIAMS, D.I.C., PH.D. and B. AALAMI, D.I.C., PH.D.*

Summary.—A Perry-Robertson strut analysis is compared to elastic orthotropic plate solutions for several initially deformed stiffened compression panels of typical cross-section, subjected to different distributions of in-plane loading. Conditions simulating the influence of longitudinal compatibility with adjacent panels, lateral constraint, shear lag and unequal end loads are considered. The influence of side ratio is considered for the case of equal uniform stress. It is concluded that the strut approach may significantly underestimate stresses involving lateral constraint, that the strut approach may not give realistic stresses in cases of varying stress due to shear lag, that a strut approach for mean stress gives reasonable solutions for cases of unequal end load for most practical cases of interest and that side ratio may affect the accuracy of strut solutions at values of length/width greater than 1.0.

LIST OF SYMBOLS

x, y, z	cartesian co-ordinates, x and y in the plane of the plate, z normal
u, v, w	plate displacements corresponding to the above axes
w_i	initial deformation at any position in the plate
w_0	initial deformation at centre plate
M_x, M_y	bending moments per unit length
M_{xy}	twisting moment per unit length
N_x, N_y	normal membrane forces per unit length
N_{xy}	membrane shearing force per unit length
D_x, D_y	flexural rigidities per unit length
D_{xy}	torsional rigidity per unit length
D_1	$\mu_x D_y = \mu_y D_x$
μ_x, μ_y	flexural Poisson's ratios
C_x, C_y	extensional stiffness per unit length
C_{xy}	membrane shearing rigidity per unit length
C_1	$\nu_x C_y = \nu_y C_x$
ν_x, ν_y	membrane Poisson's ratios
I_x, I_y, I_{xy}	effective plate inertias per unit length
I_p	inertia of isotropic plate per unit length
J_x	torsion constant of open stiffeners
Z_x, Z_y	effective section modulii per unit length
A_x, A_y, A_{xy}	effective areas per unit length
A_x^*	gross area per unit length
r_x	radius of gyration of stiffener and associated isotropic plate
E	Young's modulus
G	modulus of rigidity
K	torsion constant of trough stiffener and associated plate
μ	trough stiffener torsional stiffness reduction factor to account for local distortions
b_a, b_e	actual and effective isotropic plate width between stiffeners
a, b	plate dimensions in x and y directions
c	distance from neutral axis to extreme fibre in compression
t	thickness of isotropic plate
σ_x	average axial stress over effective area
σ_x^*	average axial stress over gross area
σ_{cr}	strut critical stress
σ_c	extreme fibre stress at centre plate
σ_m	maximum extreme fibre stress
τ	shear stress

The above definitions refer to the orthotropic plate unless specific reference is made to isotropic plate.

*Paper No. 3231, submitted by the author on October 16, 1972.

Dr. Williams is Project Engineer, Redpath Dorman Long (Contracting) Ltd, West Gate Bridge, Melbourne.

Professor Aalami is an Associate Professor, Arya Mehr University of Technology, Tehran.

INTRODUCTION

Multiple stiffened plate panels are a basic component of most large metal clad structures. The simplest method of elastic analysis of these panels when subjected to uniaxial compression, is the so called Perry-Robertson method. This method assumes that the panel behaves as an initially deformed strut. Combined surface stresses are calculated so as to include the non-linear load-deflection characteristics by way of an initial deformation magnification factor which is a function of the ratio of the applied axial load to the critical axial load.

A Perry-Robertson strut analysis is simple to apply and is known to give practical results in many instances. However, it does not allow for biaxial action of the panels or their torsional characteristics, nor does it account for the mode of application of the edge compression, and hence there are bound to be cases where a designer is in doubt as to the accuracy of the method. In this paper three parameters which could affect the degree of biaxial action are considered, namely, the stiffener/plate proportions, the edge load distribution and the side ratio. The influence of these parameters is evaluated by comparing an orthotropic plate solution with a Perry-Robertson solution for a range of typical cases. Varying flexural and torsional stiffness ratios are considered for edge loadings chosen to represent the influence of longitudinal compatibility, lateral constraint, shear lag and varying axial compression. It is proposed to extend the work at a later date to produce design data for cases where the strut approach is shown to be inadequate.

PLATE EXAMPLES

Geometry:

Fig. 1 shows the overall dimensions of the panel, the co-ordinate axes and the finite difference grid used for all solutions. In the four load case-studies the actual panel dimensions are: $a = 320.0$ cm, $b = 594.4$ cm. In the exercise to evaluate the influence of side ratio the length b is varied. Fig. 2 shows the four typical sections considered, they are representative of arrangements used in box girder bridges. Section 1 is an arrangement which might be used in conjunction with a composite deck. Sections 2 and 3 are typical flange or web arrangements. Section 4 is a typical orthotropic deck arrangement.

Edge conditions:

Two sets of edge conditions must be defined, namely, those relating to the flexural behaviour and those relating to the membrane behaviour. The membrane conditions are defined in the following section of the text

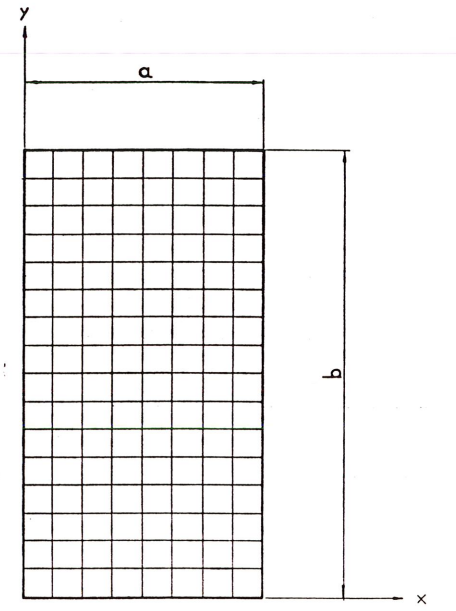

Fig. 1.—Panel showing co-ordinate axes and finite difference grid.

describing the panel loading. For the flexural conditions, simple support was assumed on all edges ($w = 0$, $\partial^2 w/\partial x^2 = 0$ along $x = 0$, a and $w = 0$, $\partial^2 w/\partial y^2 = 0$ along $y = 0$, b). This is a conservative assumption for cases where the supports or adjacent structure give rise to some degree of rotational constraint but, in cases of antisymmetric distortions in adjacent panels combined with yielding at supports due to welding, it could occur and hence must be the design condition.

Orthotropic plate properties :

The orthotropic plate properties of the above sections are given in Table I. They were computed using the following expressions:

Flexural stiffnesses: $D_x = EI_x/(1 - \mu_x \mu_y)$

$D_y = EI_y/(1 - \mu_x \mu_y)$

Torsional stiffness (Ref. 1):

(*a*) bulb stiffeners: $D_{xy} = GI_p + GJ_x/4b_a$

(*b*) trough stiffeners: $D_{xy} = \mu GK/4b_a$

In-plane axial stiffnesses: $C_x = EA_x/(1 - \nu_x \nu_y)$

$C_y = EA_y/(1 - \nu_x \nu_y)$

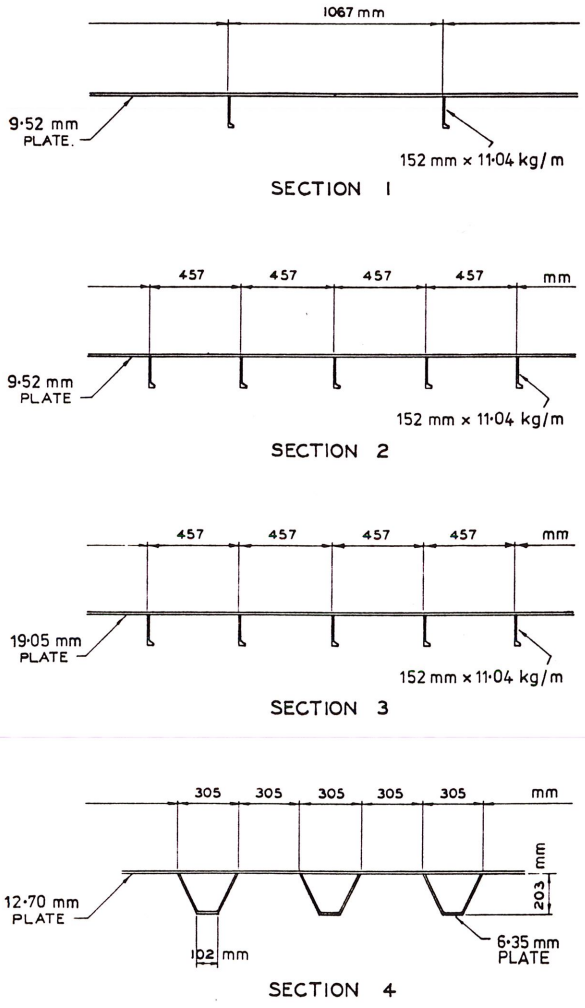

Fig. 2.—Typical cross-sections.

In-plane shear stiffness: $C_{xy} = GA_{xy}$

Poisson's ratios

(*a*) Flexural: $\mu_x = 0.3$

$\mu_y = 0$

(*b*) Membrane: $\nu_x = 0.3$

$\nu_y = 0.3\ (A_y/A_x)$

The above parameters are defined in the List of Symbols. In calculating I_x and I_y allowance was made for loss of plating effectiveness. This was computed using the expression given in BS 153 (Ref. 2) for high yield steel, thus:

$$b_e = 34t(b_a/t - 15)/(b_a/t - 12)$$

The same loss was assumed in computing A_x, A_y and A_{xy}. The values for J_x were computed by considering the bulbs as a thin plate with an attached equivalent rectangle. The value for μ was taken from Ref. 1.

The question of loss of effectiveness is in a state of flux at the moment. The Merrison Report (Ref. 3) makes the computation more rational by incorporating specified plate distortions between stiffeners and by relating the loss to the design stress level. This is a preferable approach provided the iterative nature of the method is practical from the design point of view.

TABLE I

Property	Section 1	2	3	4	Dimensions
D_x	2.37	5.42	7.23	18.4	$\times 10^6$ Nm²/m
D_y	4.29	9.72	119.8	35.4	$\times 10^3$ Nm²/m
D_{xy}	2.49	5.65	47.7	29.8	$\times 10^3$ Nm²/m
C_x	8.76	19.3	45.5	38.5	$\times 10^8$ N/m
C_y	5.78	12.8	40.3	26.3	$\times 10^8$ N/m
C_{xy}	2.27	4.90	15.1	10.2	$\times 10^8$ N/m
μ_x	0.3	0.3	0.3	0.3	
μ_y	0	0	0	0	
ν_x	0.3	0.3	0.3	0.3	
ν_y	0.2	0.2	0.26	0.21	
w_0	0.401	0.409	0.259	0.386	cm

Strut properties :

The strut properties for the four sections including the allowable loads according to BS 153, are given in Table II.

Initial deformation :

The initial deformation assumed in the BS 153 strut formula has been used in this investigation. This gives a central distortion of:

$$w_0 = \frac{0.003\, a\, r_x}{c}$$

In the above expression a is the span and r_x is the radius of gyration of the strut and c is the distance from the neutral axis to the extreme fibre in compression. This gives two values for w_0 in the case of unsymmetric sections, depending on the direction of bending. In this investigation it has been assumed that bending is such as to produce compression in the extreme fibre of the stiffeners. Specific values of w_0 are given in Table I.

In the orthotropic plate analysis a sinusoidal distribution of initial deformation of the following form has been assumed.

$$w_i = w_0 \sin \frac{\pi x}{a} \sin \frac{\pi y}{b}$$

The Merrison Report, in line with Continental practice has related stiffener distortions to the span between transverse members. Although the distinction between the direction of bending implicit in the BS 153 strut formula has been retained in the Merrison Report, it would seem logical to have also retained some relation to the stiffness of the member.

TABLE II

Section	A_x* (cm²/cm)	A_x (cm²/cm)	A_x/A_x*	I_x (cm⁴/cm)	r_x (cm/cm)	a/r_x (cm)	σ_x (MPa)	σ_x* (MPa)
1	1.084	0.411	0.38	11.44	2.076	154.2	156.0	58.7
2	1.260	0.925	0.73	26.33	2.101	152.4	156.0	114.3
3	2.212	2.212	1	34.94	1.565	204.5	122.0	122.0
4	1.849	1.849	1	89.13	2.733	117.1	173.0	173.0

LOADING CASES

Fig. 3 shows the five loading cases applied to each of the sections described in the preceding text. These are the membrane edge conditions. The orthotropic plate analysis requires the definition of two membrane conditions on each edge, namely a normal stress or displacement and a tangential stress or displacement. Where no applied condition is shown in Fig. 3, zero stress has been specified in the analysis.

Loadcase 1 is the most elementary condition considered and could be expected to give the nearest agreement with a strut analysis. The other four cases represent practical variations from this idealised condition; they would occur in some combination in practice.

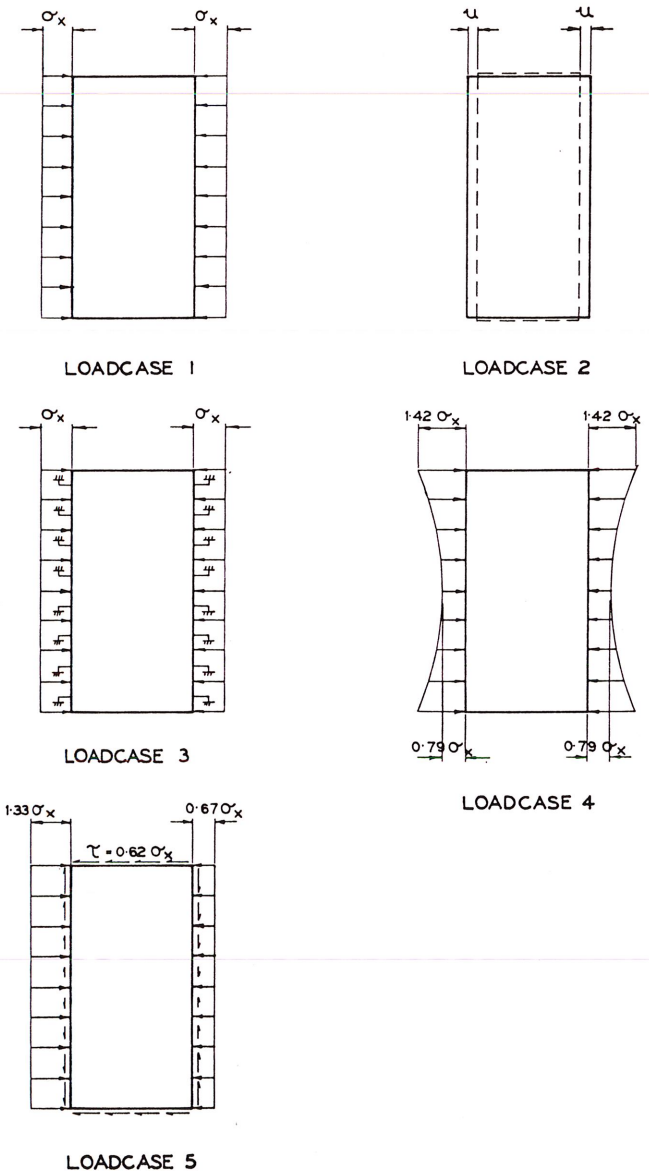

Fig. 3.—Typical compression panel load conditions.

If there were no out-of-plane deformation (plane stress) loadcase 2 would be identical to loadcase 1. Because of the initial deformation however, there is out-of-plane deformation and loadcase 1 will result in some degree of non-uniform in-plane edge displacement which is incompatible with an adjacent panel. Compatibility is implicit in loadcase 2 which, in this respect, is more realistic than loadcase 1.

The axial rigidity of transverse members at the loaded ends of a compression panel exerts some degree of tangential membrane restraint on the panel. In loadcase 3 the loaded edges are fixed against tangential displacement, representing a completely rigid connection. In practice the fixity would be reduced by residual stresses in the case of a welded connection and slip in the case of a bolted connection so that the results will give an upper bound to the effect of tangential constraint.

Loadcase 4 represents the variation in axial stress between webs of a girder due to shear lag. A variation of the order shown is representative of actual cases at a pier in a box girder bridge. Design data on shear lag, including the influence of stiffeners is, unfortunately, rather limited. In view of the severity of the effect this is an area requiring urgent attention.

Loadcase 5 represents the variation in axial compression along the length of a panel which would occur in the flange of a box girder due to variation in bending moment. The co-existent shear forces are assumed to be constant along the unloaded sides and to vary linearly across the loaded ends.

ANALYSIS

Perry-Robertson strut :

The maximum extreme fibre compressive stress due to axial load occurs at centre-span and is given by the expression:

$$\sigma_c = \sigma_x + \frac{\sigma_x A_x w}{Z_x}$$

where: $w = \dfrac{w_0}{(1 - \sigma_x/\sigma_{cr})}$

σ_x = applied axial compressive stress on effective area

σ_{cr} = strut critical stress = $\pi^2 E/(a/r_x)^2$

A_x = effective area per unit width

$Z_x = I_x/c$ = effective section modulus per unit width

This expression is only valid for elastic behaviour and assumes that the load is concentric at the ends.

Orthotropic plate analysis :

The orthotropic plate results were obtained from a computer program which uses dynamic relaxation to solve finite difference approximations to the large deflection orthotropic plate equations including initial out-of-plane displacements. The equations and a brief description of the method of solution are given in the Appendix.

RESULTS

Average stress :

Stresses given by the various orthotropic plate solutions are compared to centre span extreme fibre compressive stress given by the corresponding Perry-Robertson solution for average axial stress in each case. The average axial stress for loadcase 1, 3, 4 and 5 is shown in Fig. 3. For loadcase 2 the average is the mean value along the loaded edge corresponding to the particular value of uniform displacement. In the figures the average axial stress is specified as the stress on the gross area of the cross-section (σ_x*).

Orthotropic plate stresses :

The orthotropic plate solution gives values for displacements (u, v, w), moments (M_x, M_y, M_{xy}) and axial forces (N_x, N_y, N_{xy}) at each node. The combined longitudinal stresses can then be computed using the expression

$$\sigma = \frac{N_x}{A_x} \pm \frac{M_x}{Z_x}$$

Where, N_x and M_x are the longitudinal axial force and moment per unit width respectively, and A_x and Z_x are the longitudinal effective area and effective section modulus per unit width respectively. Two stresses given by the orthotropic plate solutions are plotted, σ_c the compressive stress at centre-panel and σ_m the maximum compressive stress. In some cases the maximum compressive stress occurs at centre panel, $\sigma_c = \sigma_m$.

Effect of type of loading :

Figs. 4, 5, 6 and 7 give results for the five types of loading applied to the 320.0 cm × 594.4 cm panels for sections 1, 2, 3 and 4 respectively. The loadcases are indicated by number and the corresponding Perry-Robertson solution is designated P.R.

Loadcase 1 and 2.—Maximum stress occurs at centre span for all sections ($\sigma_m = \sigma_c$) and agrees within 1% of the corresponding Perry-Robertson solution. The variation in stress along the loaded edge for loadcase 2 does not exceed 1% for the load range covered.

The lack of load shedding is due to the relatively low out-of-plane displacement combined with the weak biaxial plate properties. The small out-of-plane deflexion relative to plate geometry is apparent in the results showing convergence referred to in the Appendix. The capacity to shed load is an important consideration in regard to the ultimate load capacity. If a centrally located stiffener, having yielded, sheds additional load to adjacent stiffeners rather than over the panel width the

ultimate load will not be much greater than the capacity of a single stiffener.

Loadcase 3.—For all sections except 1, maximum stress occurs at centre span. In the case of section 1 the maximum stress begins to move away from the centre at about $\sigma_x^* = 108$ MPa. The Perry-Robertson solution underestimates the maximum stress for all sections such that the load factor on yield for the respective allowable stresses given in BS 153 is reduced from 1.7 to 1.6 for sections 1, 2 and 4 and to 1.55 for section 3. The greater sensitivity of section 3 reflects its significantly greater relative transverse stiffness.

Loadcase 4.—For sections 1, 2 and 4 the maximum stress is located in the corner for the full load range and is a membrane stress equal to the applied stress at the corners ($1.42\sigma_x$). For section 3 the maximum is located at the corners up to an average stress of about $\sigma_x^* = 105$ MPa above which non-linear bending effects become significant and the maximum moves towards the centre. A direct comparison between the maximum stresses and the respective Perry-Robertson solutions for average axial stress and maximum (central) initial deformation is not really meaningful except as a guide to the order of magnitude of the error involved in a Perry-Robertson analysis. At the allowable (BS 153) design load the order of this error is 16%, 14%, 0% and 12% for sections 1, 2, 3 and 4 respectively. The marked difference between the percentages for sections 1, 2 and 4 and the percentage for section 3 reflects the influence of slenderness ratio on the respective Perry-Robertson solutions. The centre panel stresses agree almost exactly with Perry-Robertson solutions for $0.79\sigma_x$, the applied stress acting in line with the longitudinal centre-line.

Loadcase 5.—The centre panel stress agrees within 1% with the Perry-Robertson solution for all sections but is not the maximum, which originates near the edge on the longitudinal centre-line and moves in towards the centre as the load increases. The yield stress load factor on the BS 153 allowable stresses are 1.60, 1.63, 1.66 and 1.54 for sections 1, 2, 3 and 4 respectively. As in the case of loadcase 3 the relative magnitudes of these factors reflect the influence of the respective slenderness ratios. The higher the slenderness ratio, the more rapid the growth of the proportion of extreme fibre stress due to bending and the quicker the influence of membrane stress concentration at one end is dissipated. In practice the difference in end loads would not be so severe in the highly stressed areas and the significance of this effect would be considerably reduced.

Effect of side ratio :

Fig. 8 illustrates the effect of side ratio for section 2, subjected to loadcase 1 for an average stress $\sigma_x^* = 114$ MPa (equal to 156 MPa on the effective area, the allowable according to BS 153). Two side edge ($y = 0, b$) membrane conditions are considered, edges stress free ($\sigma_y = 0$, $\tau = 0$) and edges restrained normally ($v = 0$, $\tau = 0$). The flexural edge conditions are simple support on all edges.

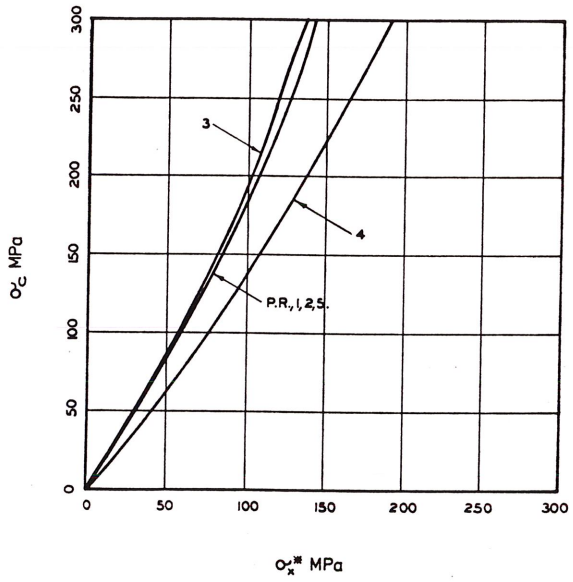

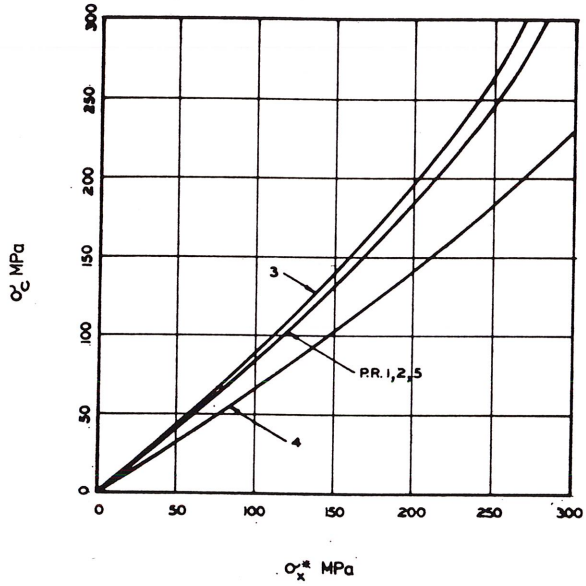

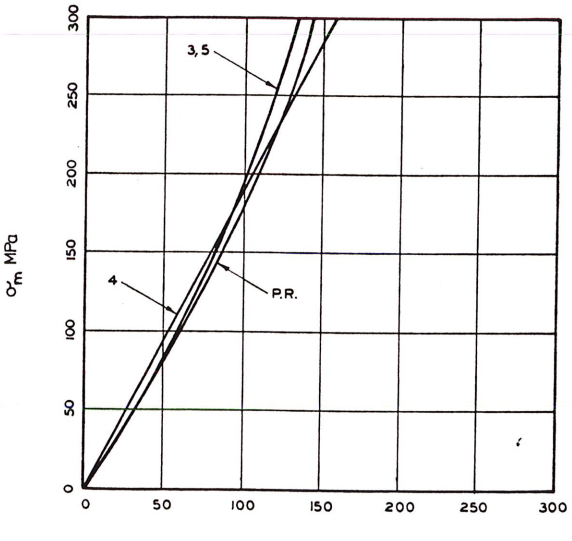

Fig. 4.—Stresses: Section 1.

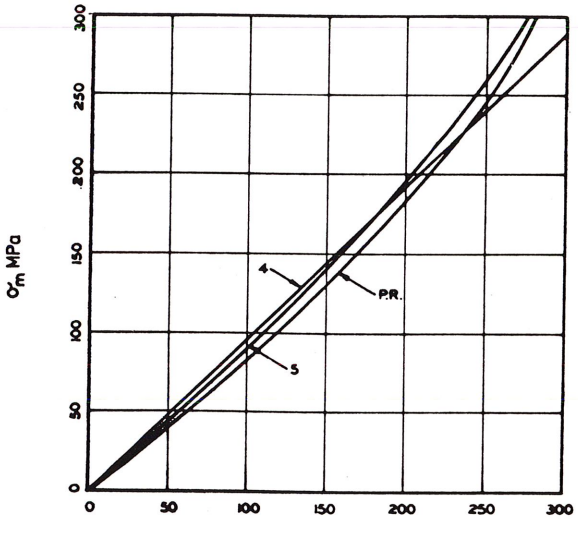

Fig. 5.—Stresses: Section 2.

In the stress free case, the influence of vertical side support is sufficient to significantly influence stresses for side ratios less than about $b/a = 0.5$. In the edges restrained case the restriction of Poisson expansion causes an increase in stresses compared to the edges stress free case, for side ratios up to about $b/a = 1.25$. The counteracting effect of inward movement of the sides due to out-of-plane displacement causes the reversal of the influence of side restraint at a side ratio of about 0.5.

For the panel geometry of the case considered the accuracy of the orthotropic idealisation is questionable below a side ratio of about 0.5 although the trends observed are thought to be realistic. In practice the edge conditions will approximate the stress free case more closely, depending on the position of the panel in the structure and on the in-plane stiffness of boundary members.

CONCLUSIONS

1. The relatively small out-of-plane deflections (including initial distortions), and the strong uniaxial characteristics of stiffened panels inhibit load shedding at design load levels and hence the panel behaviour is insensitive to the lack of longitudinal compatibility implicit in the uniform applied stress load condition.

2. Lateral constraint at transverse supports can significantly reduce the yield load factor on the allowable load according to BS 153. The sensitivity to this effect increases as the transverse to longitudinal membrane stiffness ratio increases.

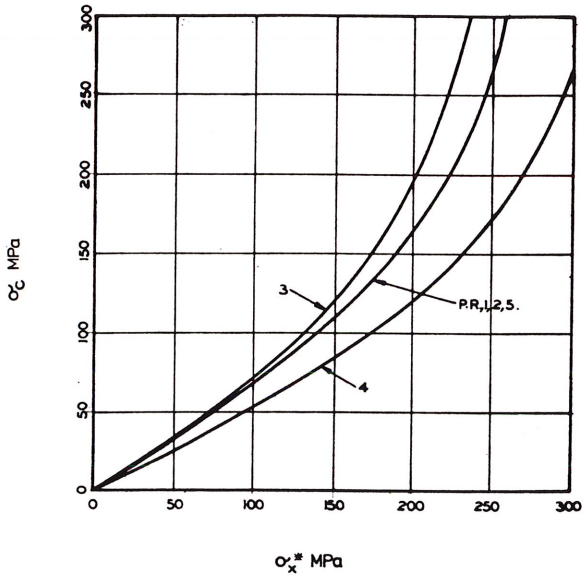

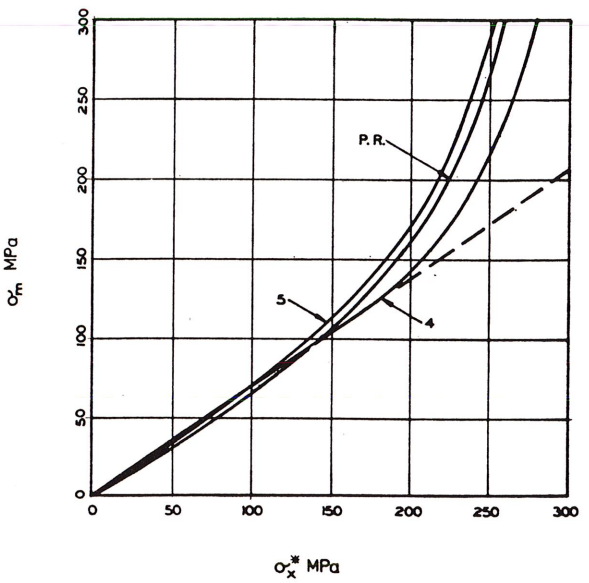

Fig. 6.—Stresses: Section 3.

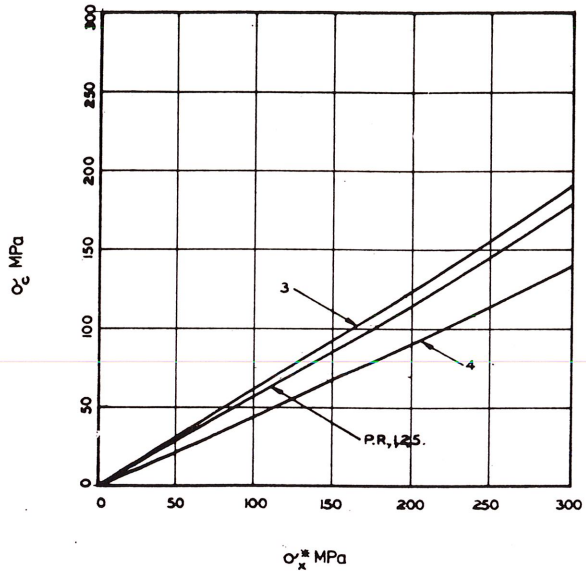

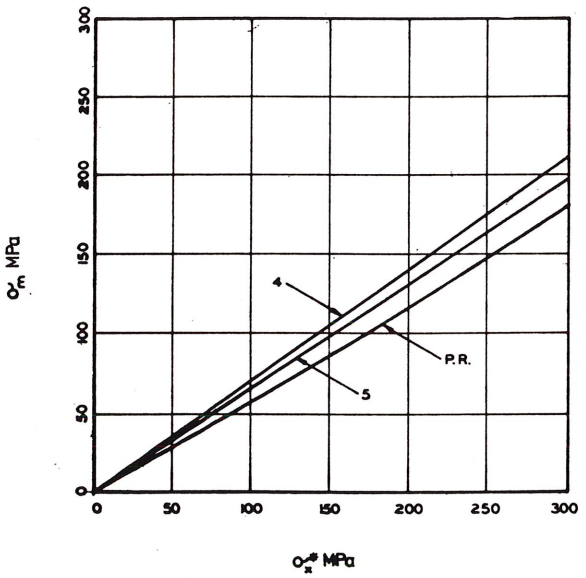

Fig. 7.—Stresses: Section 4.

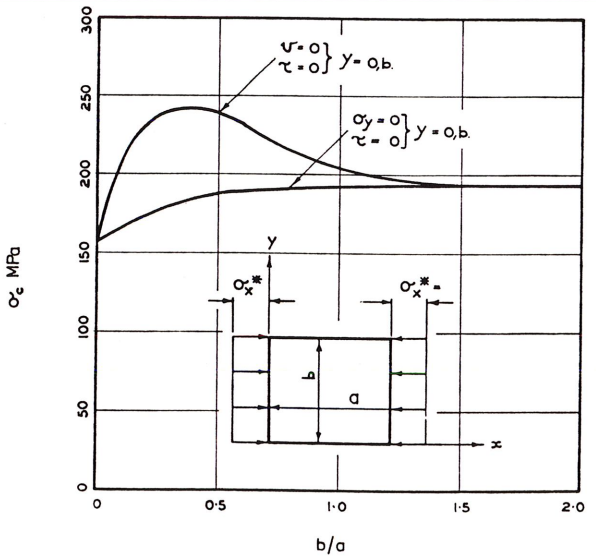

Fig. 8.—Effect of side ratio; Section 2, Loadcase 1.

3. The practice of designing compression flange panels located in areas of significant transverse variation in longitudinal stress due to shear lag as initially deformed struts subjected to the maximum stress occurring at flange/web junctions, is unrealistic and conservative. This effect becomes more pronounced as slenderness ratio increases and design data is required to indicate when allowances can be made in practice.

4. Unequal load at either end of a panel due to variation in beam bending moment can reduce the yield load factor according to BS 153. However, in regions of maximum stress the variation in load between the end of a panel is unlikely to be of the order considered as part of this investigation and hence a Perry-Robertson analysis for average stress will usually be adequate. The sensitivity to this effect diminishes as slenderness ratio increases.

5. Side ratio may have a significant adverse effect on stress for panels with a loaded edge length less than the unloaded edge length if lateral expansion is prevented. The effect is conservative if the sides are free to expand and becomes significant when the loaded edge length is less than half the unloaded edge length.

ACKNOWLEDGMENTS

This work was carried out as part of a programme of research into the behaviour of stiffened steel plate at the Imperial College, sponsored by the British Steel Corporation under the general direction of Dr J. C. Chapman.

References

1. American Institute of Steel Construction—*Design Manual for Orthotropic Steel Plate Deck Bridges.*
2. British Standards Institution—*Specification for Steel Girder Bridges.* BS 153:1958. Parts 3B and 4.
3. Gt. Britain. Dept of the Environment—*Criteria for the Assessment of Steel Box Girder Bridges with particular reference to the Bridges at Milford Haven and Avonmouth,* 1972.
4. Von Karman, Th.—Festigkeitsprobleme im Maschinenbau. *Encyklopaedie der Mathematischen Wissenschaften,* 1910, Vol. IV.
5. Lekhnitskii, S. G.—Anisotropic Plates. *Gostekhizdat,* 1947.
6. Soper, W. G.—Large deflexion of stiffened plates. *Jour. Appl. Mech.,* Dec., 1958.
7. Maguerre, K.—Zur Theorie der gekruemmter Platte grosser Formaenderung. *Proc. Fifth Int. Congress Appl. Mech., Cambridge,* 1938.
8. Aalami, B. and Chapman, J. C.—Large Deflexion Behaviour of Rectangular Orthotropic Plates. *Proc. I.C.E.,* Vol. 42, March, 1969.
9. Rushton, K. R.—Large Deflexion of Variable-Thickness Plates. *Int. Jour. Mech. Sci.,* Vol. 10, 1968.
10. Rushton, K. R.—Postbuckling of Tapered Plates. *Int. Jour. Mech. Sci.,* Vol. 11, 1969.
11. Otter, J. R. H., Cassel, A. C. and Hobbs, R. E.—Dynamic Relaxation. *Proc. I.C.E.,* Vol. 35, Dec., 1966.
12. Day, A. S.—Analysis of Plates by Dynamic Relaxation with special reference to Boundary Conditions. *Int. Symposium Use of Digital Computers in Structural Engg., Univ. of Newcastle-upon-Tyne, July,* 1966.
13. Rushton, K. R.—Dynamic Relaxation Solutions of Plate Problems. *Int. Jour. Strain Analysis,* Vol. 3, 1969.

APPENDIX

The results given in this paper were obtained from a computer program which uses dynamic relaxation to solve first-order finite difference approximations to the elastic large deflection equations (Ref. 4) modified to take account of orthotropy (Refs. 5 and 6) and initial out-of-plane deformation (Ref. 7). For positive directions of forces as shown in Fig. 9, the equations are as follows:

$$\frac{\partial^2 M_x}{\partial x^2} - 2\frac{\partial^2 M_{xy}}{\partial x \partial y} + \frac{\partial^2 M_y}{\partial y^2} + N_x \frac{\partial^2}{\partial x^2}(w + w_0) + 2N_{xy}\frac{\partial^2}{\partial x \partial y}(w + w_0) + N_y \frac{\partial^2}{\partial y^2}(w + w_0) = \rho_w \left(\frac{\partial w}{\partial t} + \frac{K_w}{\Delta t} w\right) \tag{A1}$$

$$\frac{\partial N_x}{\partial x} + \frac{\partial N_{xy}}{\partial y} = \rho_u \left(\frac{\partial u}{\Delta t} + \frac{K_u}{\Delta t} u\right) \tag{A2}$$

$$\frac{\partial N_y}{\partial y} + \frac{\partial N_{xy}}{\partial x} = \rho_v \left(\frac{\partial v}{\Delta t} + \frac{K_v}{\Delta t} v\right) \tag{A3}$$

$$M_x = -\left(D_x \frac{\partial^2 w}{\partial x^2} + D_1 \frac{\partial^2 w}{\partial y^2}\right) \tag{A4}$$

$$M_y = -\left(D_y \frac{\partial^2 w}{\partial y^2} + D_1 \frac{\partial^2 w}{\partial x^2}\right) \tag{A5}$$

$$M_{xy} = 2 D_{xy} \frac{\partial^2 w}{\partial x \partial y} \tag{A6}$$

$$N_x = C_x\left(\frac{\partial u}{\partial x} + \frac{1}{2}\left(\frac{\partial w}{\partial x}\right)^2 + \frac{\partial w}{\partial x}\frac{\partial w_0}{\partial x}\right) + C_1\left(\frac{\partial v}{\partial y} + \frac{1}{2}\left(\frac{\partial w}{\partial y}\right)^2 + \frac{\partial w}{\partial y}\frac{\partial w_0}{\partial y}\right) \tag{A7}$$

$$N_y = C_y\left(\frac{\partial v}{\partial y} + \frac{1}{2}\left(\frac{\partial w}{\partial y}\right)^2 + \frac{\partial w}{\partial y}\frac{\partial w_0}{\partial y}\right) + C_1\left(\frac{\partial u}{\partial x} + \frac{1}{2}\left(\frac{\partial w}{\partial x}\right)^2 + \frac{\partial w}{\partial x}\frac{\partial w_0}{\partial x}\right) \tag{A8}$$

$$N_{xy} = C_{xy}\left(\frac{\partial u}{\partial y} + \frac{\partial v}{\partial x} + \frac{\partial w}{\partial x}\frac{\partial w}{\partial y} + \frac{\partial w}{\partial x}\frac{\partial w_0}{\partial y} + \frac{\partial w}{\partial y}\frac{\partial w_0}{\partial x}\right) \tag{A9}$$

The boundary conditions for which solutions are presented are given below. They apply along $x = a$, similar conditions apply along $y = b$.

Simply supported edges:

(*a*) flexural

$$w = 0$$

$$\frac{\partial^2 w}{\partial x^2} = 0$$

(*b*) membrane

(i) applied loads:

N_x = applied value

N_{xy} = applied value

$$\frac{\partial u}{\partial x} = \frac{N_x}{C_x} - \frac{1}{2}\left(\frac{\partial w}{\partial x}\right)^2 - \frac{\partial w}{\partial x}\frac{\partial w_0}{\partial x} - \frac{C_1}{C_x}\frac{\partial v}{\partial y}$$

$$\frac{\partial v}{\partial x} = \frac{N_{xy}}{C_{xy}} - \frac{\partial u}{\partial y}$$

(ii) applied displacements:

u = applied value

v = applied value

$$\frac{\partial u}{\partial x} = 0$$

$$\frac{\partial v}{\partial x} = 0$$

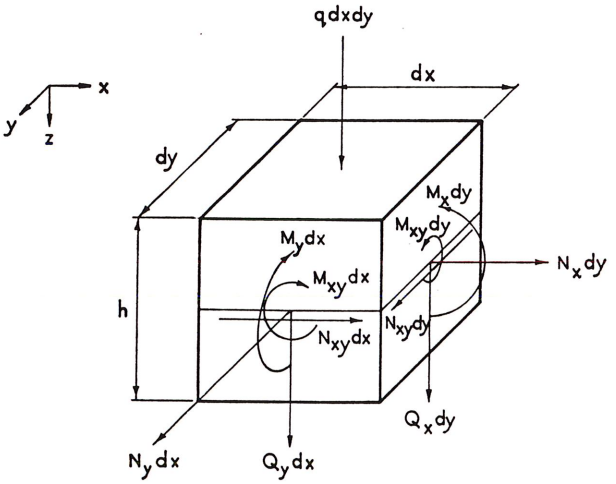

Fig. 9.—Positive directions of forces.

Solutions to the equations have previously been obtained by Aalami (Ref. 8) using direct Gaussian reduction of the finite difference equations. Results were restricted however because the numerical technique failed to converge at loads of the order of the critical load. Rushton (Refs. 9 and 10) showed that this problem was overcome by the iterative dynamic relaxation method, and his work has been extended to evaluate the influence of initial distortions.

The values of the right-hand-side of equations (A1), (A2) and (A3) relate to the dynamic relaxation method. The method is discussed in detail in Refs. 11, 12 and 13 and therefore only a brief summary will be given. Dynamic relaxation is an iterative method involving the vibration characteristics of the plate. The right hand terms referred to above include an acceleration term and a viscous damping term. If the damping coefficients are chosen to give critical damping, oscillations will die out after about $3N$ iterations where N is the number of iterations in one complete cycle. Once oscillations cease, the final displacements and forces are the required static solution to the differential equations. Critical damping factors and the number of iterations per oscillation for each mode of vibration (u, v and w) can be obtained by monitoring the behaviour of the displacements with zero damping.

Fig. 10 is a typical example of convergence behaviour for the cases studied in this paper. All the results given in Figs. 4 to 7 are for a mesh size of $I = 8$, $J = 16$ for which Fig. 9 shows an accuracy of about 1%.

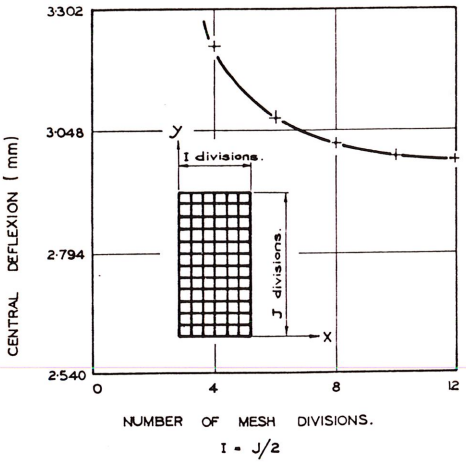

Fig. 10.—*Typical convergence behaviour; Section* 2, *Loadcase* 2.